DESY 97–121
DAPNIA–SPP 97–14
MSUHEP–70606
CTEQ–707

Summary of Working Group I: Hadron Structure [1]

J. Blümlein[a], J. Huston[b], C. Royon[c] and R. Yoshida[d]

[a] *DESY-Zeuthen, Platanenallee 6, D-15735 Zeuthen, Germany*
[b] *Department of Physics and Astronomy, Michigan State University, East Lansing, MI 48824–1116, USA*
[c] *DAPNIA-SPP, Centre d'Etudes de Saclay, F-91191 Gif-sur-Yvette Cedex, France*
[d] *Argonne National Laboratory, Argonne, IL 60439, USA*

Abstract. A summary is given on the main aspects which were discussed by the working group. They include new results on the deep inelastic scattering structure functions F_2, xF_3, F_L and $F_2^{c\overline{c}}$ and their parametrizations, the measurement of the gluon density, recent theoretical work on the small x behavior of structure functions, theoretical and experimental results on α_s, the direct photon cross section, and a discussion of the event rates in the high p_T range at Tevatron and the high Q^2 range at HERA, as well as possible interpretations.

INTRODUCTION

Since the last International Conference on Deep Inelastic Scattering at Rome in April 1996 various new experimental and theoretical results have been obtained on the behavior of the structure functions in deeply inelastic scattering and related quantities. New measurements were performed for $F_2(x,Q^2)$ in the low Q^2 domain, for $F_L(x,Q^2)$, and $F_2^{c\overline{c}}(x,Q^2)$. Furthermore a refined analysis was carried out for the structure functions in deep-inelastic neutrino scattering. On the theoretical side, further investigations of the small x behavior of structure functions were carried out and various studies on the description of their heavy flavor contributions were performed. Several very advanced higher order calculations were carried out, among them the 4–loop correction for the QCD β–function in the $\overline{\rm MS}$ scheme. Different new measurements of the strong coupling constant $\alpha_s(M_Z)$ were performed.

[1] Summary talk given at the DIS97 conference, Chicago, 14-18 April 1997

The HERA experiments H1 and ZEUS have now accumulated a substantial statistics in the high Q^2 range, $Q^2 > 10000\,\mathrm{GeV}^2$. As a surprise both experiments found an indication for an excess of events in this kinematic range over the rate predicted by the Standard Model, which was firstly reported in February this year. Very intense theoretical investigations followed in the few weeks shortly after and experimental searches for signatures at Tevatron, which could be related, were performed. In the following we will give a summary on these aspects which were discussed by the working group on Hadron Structure.

NUCLEON STRUCTURE FUNCTION MEASUREMENTS

Results of deep inelastic structure function measurements from NMC, CCFR, and the HERA experiments were presented for $F_2^{ep}(x,Q^2)$, $F_2^{\nu N}(x,Q^2)$, $xF_3^{\nu N}(x,Q^2)$, $F_L(x,Q^2)$, and $F_2^{c\bar{c}}(x,Q^2)$ [1–6].

$F_2^{ep}(x,Q^2)$ at low Q^2

The ZEUS and H1 collaborations have now measured F_2 down to Q^2 as low as 0.1 GeV^2 and x as low as a few times 10^{-6} [1,2]. Figure 1 shows the HERA results, as well as the measurement from E665, in terms of the total virtual photon-proton cross section $\sigma(\gamma^* p)$ versus W^2, the center of mass energy squared of the photon-proton system. Data for real photoproduction (Q^2=0) are also shown. The agreement between the measurements from the two HERA experiments is rather good. The data show a smooth transition from a slow growth of the cross section with W^2 of the real photoproduction data to a fast rise at higher Q^2 corresponding to the rise of F_2 at low x. The fits to the HERA F_2 data using the next-to-leading order (NLO) QCD evolution equations have been shown to work to an unexpectedly low value of Q^2 of $\sim$1 GeV^2 [7,8]. Also shown in figure 1 are model predictions from Donnachie and Landshoff [9], based on Regge phenomenology, as well as those of Glück, Reya and Vogt [10], based on perturbative QCD. These give a reasonable description at the lowest Q^2 and $Q^2 \gtrsim 1$ GeV^2, respectively.

$F_2^{\nu N}(x,Q^2)$ and $xF_3^{\nu N}(x,Q^2)$

The CCFR collaboration presented an updated analysis [4] of data from neutrino scattering on iron with an improved estimate of quark model parameters and systematic errors. This analysis supersedes a previous extraction of structure functions [11] in which a Monte Carlo technique was used to attempt to reduce the errors on the relative calibration between the hadron and muon

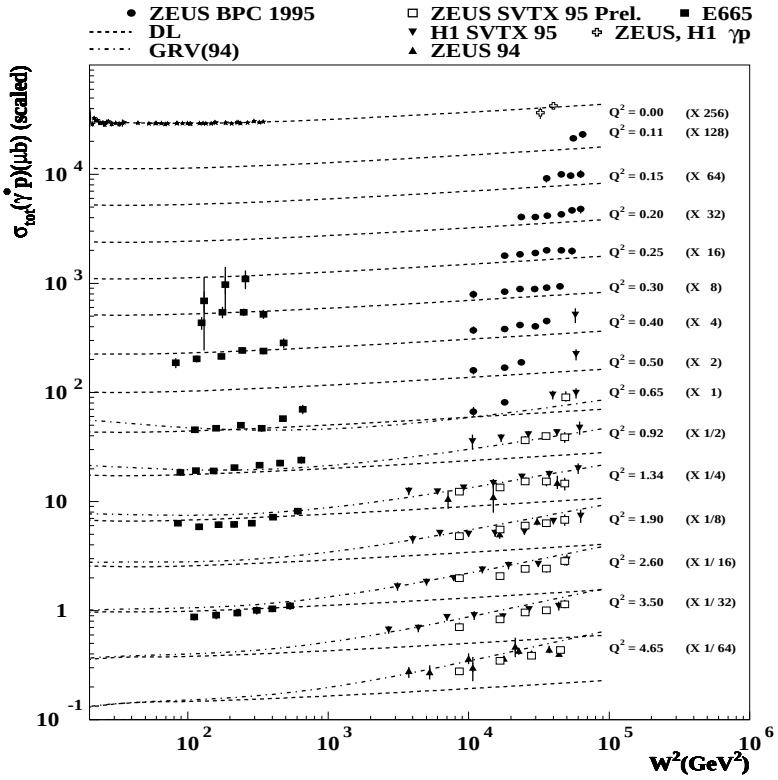

Figure 1: Virtual photon-proton cross section measurements at low Q^2, see text.

energies. The re-analysis uses the calibration directly from the test beam data taken during the course of the experiment. The net result is a change of +2.1% in the relative calibration and an increase in the corresponding systematic error to 1.4%.

The structure functions F_2 and xF_3 are extracted making corrections to an isoscalar target, no strange sea, charm mass $m_c = 0$, and removes the QED radiative corrections and propagator Q^2 dependence. After correcting for quark-charge and heavy-target effects, the CCFR results agree well with those from the NMC, E665, SLAC and the BCDMS experiments for x values greater than 0.1. For x values less than 0.1, however, the F_2 of CCFR is systematically higher, with the discrepancy reaching 15% at a x of 0.0125. These differences were also present in the previous analysis.

The discrepancy between CCFR and NMC [3] at low x is outside the experimental systematic errors quoted by both groups. One possibility is that the heavy nuclear target corrections in this region may be different between neutrinos and charged leptons. This issue can only be resolved with more experimental data.

F_L and R Measurements

The NMC collaboration has presented [3] their results on the measurement of R [12], in the low Q^2 kinematic domain ($1.2 \leq Q^2 \leq 22$ GeV^2). A measurement at even lower values of x was performed by the H1 collaboration [5,6]. In the one photon exchange approximation, the inclusive cross section reads

$$\frac{d^2\sigma}{dxdQ^2} = \frac{2\pi\alpha^2}{Q^4 x}\left(2 - 2y + \frac{y^2}{1+R}\right) F_2(x, Q^2), \qquad (1)$$

with $R = F_L/(F_2 - F_L)$. At large y, the weights of F_2 and F_L in this equation become comparable.

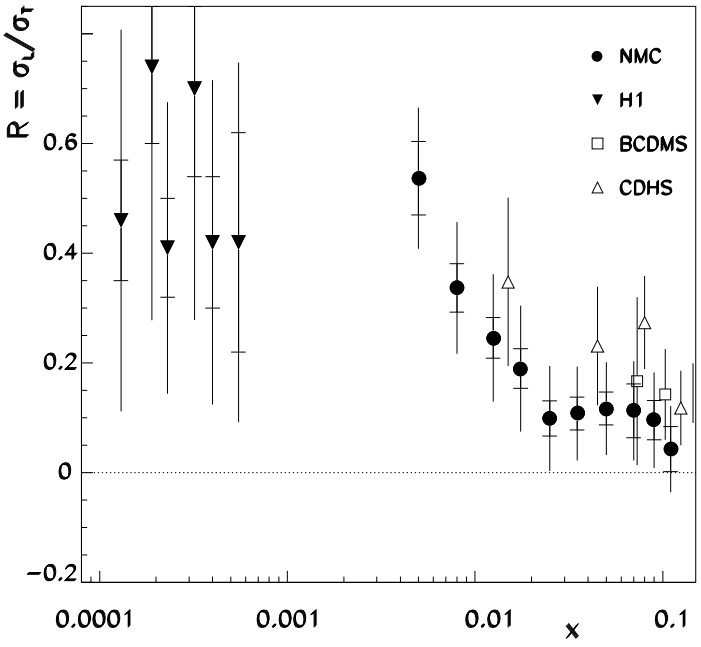

Figure 2: Measurements of R from NMC and H1, see text.

The H1 collaboration has first measured the cross section at low y where R becomes negligible in eq. (1). The structure function F_2 obtained in this region was then calculated using the NLO QCD evolution equations to larger values of y. Measuring the cross section at large y allows the determination of R [6]. The results are at much lower x than the NMC measurements and are in good continuity with them within the H1 error bars, which are still large, cf. Figure 2.

In order to determine R without assumptions, one needs to measure the cross sections at different values of y fixing the values of x and Q^2. This

requires cross section measurements at different values of the center of mass energy, implying a change of beam energies. A direct change of the beam energies at HERA has been widely discussed [13,14], but is in conflict with the accumulation of integrated luminosity. Another method would consist in the use of radiative events where a real photon is emitted in the initial state by the electron which reduces the beam energy [15,16]. However, the systematic errors are expected to be higher within this method as compared to the measurement with a lowered beam energy. With these measurements, which in principle could be performed in the near future, it may be possible to explore the structure of F_L in the low x range [17].

Charm Contribution to $F_2(x, Q^2)$

The data collected by the ZEUS and H1 experiments has allowed a measurement of the charm component to the proton structure function $F_2^{c\bar{c}}$ [18,19,5]. Compared to the previous EMC measurements, the 1994 HERA data allowed an extension of the kinematic domain by two orders of magnitude (down to $x \sim 3 \cdot 10^{-4}$ for $Q^2 \sim 7$ GeV^2) and show a steep rise of $F_2^{c\bar{c}}$ with decreasing x. The new preliminary 1995 data shown by the ZEUS collaboration reach even lower values of Q^2 and x ($Q^2 \sim 3$ GeV^2 and $x \sim 10^{-4}$). The H1 and ZEUS data are in good agreement as illustrated in Figure 3. These data also agree with the results of the NLO QCD fits performed by both collaborations. The charm treatment [20,5] in the NLO fits is the same for both experiments describing $F_2^{c\bar{c}}(x, Q^2)$ by the boson–gluon fusion process in NLO [21] assuming three light flavors. It should be noted that the dominant theoretical uncertainty in the $F_2^{c\bar{c}}$ measurement arises from the unknown charm mass.

Gluon Extraction from Structure Functions

The gluon density can be measured from the scaling violations of the structure function $F_2(x, Q^2)$. The results of QCD fits in NLO from H1 and ZEUS are shown in Figure 4. The error bands due to the statistical and systematic errors are also shown. Both of these fits use the fixed flavor number scheme (see above) for handling the charm quark. In the case of the H1 analysis, NMC and BCDMS data along with their own data are used in the fit. For the ZEUS fit, only NMC and ZEUS data are used.

The form of the parametrizations for the singlet, non–singlet and gluon distributions are somewhat different between the ZEUS and H1 fits [20,5,7]. The two results agree within their errors but the H1 fit is systematically higher than the ZEUS fit. The prospects to further constrain the gluon density in the future are discussed below [20].

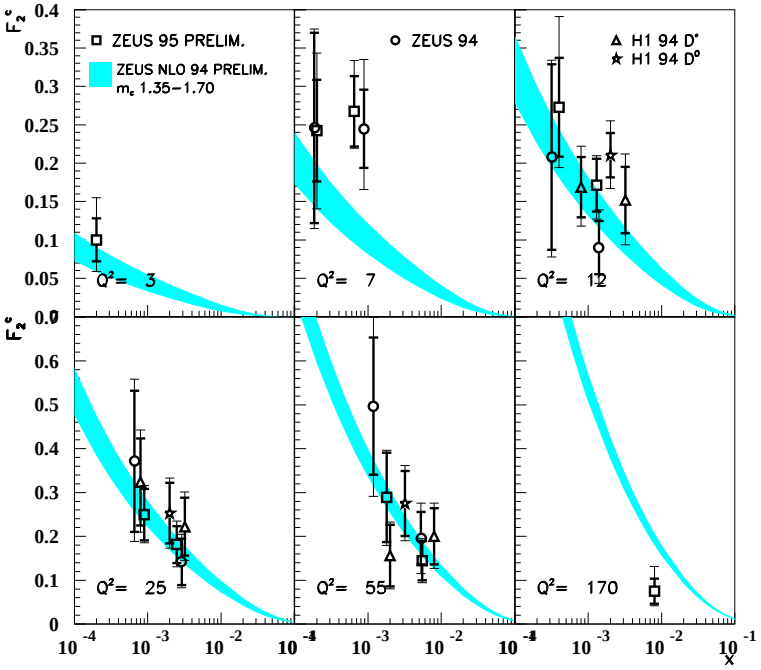

Figure 3: Measurements of $F_2^{c\bar{c}}/x, Q^2)$ from ZEUS and H1, see text.

PARTON PARAMETRIZATIONS AND HEAVY FLAVOR

Different updates of the parton parametrizations were reported during this workshop [22,23] which extend earlier analyses accounting for more dynamical effects in the heavy flavor sector. Similar aspects were considered before as well in [10] applying the coefficient functions [21] in a scenario based on three light flavors. During the last year more theoretical calculations of the heavy flavor contributions to both the structure functions in neutral and charged current deep inelastic scattering were performed [24–26] and others are in progress [27]. The data on $F_2^{c\bar{c}}(x, Q^2)$ will further improve when more luminosity is collected. This will allow for more detailed comparisons between the still somewhat different theoretical predictions in the future.

For the small x range at HERA, an effective parametrization of the structure function $F_2^{ep}(x, Q^2)$ was derived [28]

$$F_2(x, Q^2) = m \log\left(\frac{x_0}{x}\right) \log\left(1 + \frac{Q^2}{Q_0^2}\right), \qquad (2)$$

which updates an earlier analysis [29]. This representation depends only on three parameters, $m = 0.455$, $x_0 = 0.04$ and $Q_0^2 = 0.55\,\mathrm{GeV}^2$, in the range

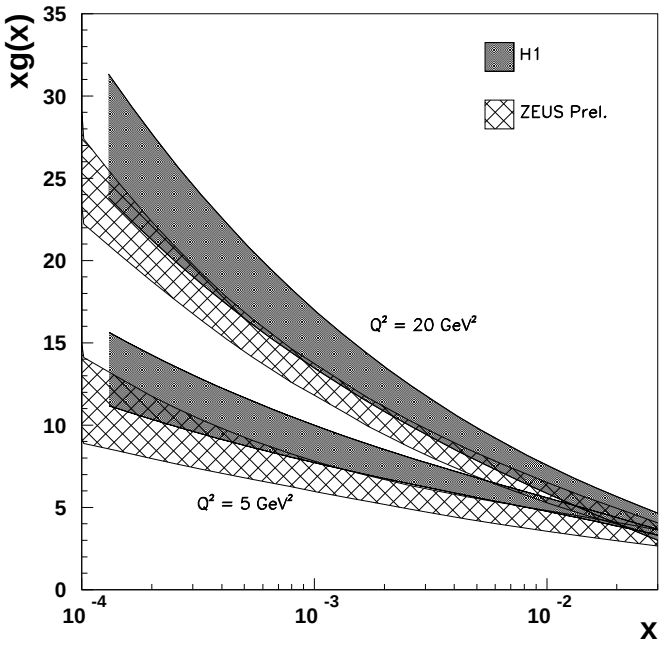

Figure 4: Gluon density distributions from H1 and ZEUS NLO QCD fits to their 1994 F_2 data, see text.

$x < 0.005$ and the whole range of Q^2. F_2^{ep} exhibits a *logarithmic* x dependence, and so far no power behavior is indicated.

In another contribution [30], a model for the low Q^2 behavior of F_2^{ep} was presented. This model aims on a description of the transition from the deep-inelastic to the real photon region and describes very well part of the data. Still an improvement is needed to match also the very recent HERA data at $Q^2 \approx 0$ [1,2].

STRUCTURE FUNCTIONS AT SMALL X

A unified BFKL-GLAP approach for the deep inelastic structure functions was presented by Kwiecinski et al. [31]. Among various possibilities of such a description one well-known way consists in relating the gluon-induced parts of the structure functions to the un-integrated gluon density $f_g(z, k_T^2)$. In earlier studies, cf. e.g. [32], however, problems were encountered in the infrared region, $k_T^2 \to 0$, requesting cut–off procedures with a strong parametric dependence. A solution to this problem was given in ref. [33] where the representation

$$F_{2,L}^g(x,Q^2) = \int_x^1 \frac{dz}{z} \int_0^{k_T^{2,max}} \frac{dk_T^2}{k_T^2} \widehat{F}_{2,L}^g(z,k_T^2,Q^2) f_g\left(\frac{x}{z},Q^2\right)$$
$$= \int_x^1 \frac{dz}{z} \widehat{F}_{2,L}^g(z,0,Q^2) G\left(\frac{x}{z},Q_0^2\right)$$
$$+ \int_x^1 \frac{dz}{z} \int_{Q_0^2}^{k_T^{2,max}} \frac{dk_T^2}{k_T^2} \widehat{F}_{2,L}^g(z,k_T^2,Q^2) f_g\left(\frac{x}{z},Q^2\right) + O\left(\frac{Q_0^2}{Q^2}\right) . \quad (3)$$

was used. For F_2 the collinear singularity has to be subtracted as in the case of collinear factorization. If one assumes $Q^2 \gg Q_0^2$ the dependence of $F_{2,L}(x,Q^2)$ in eq. (3) on Q_0^2 is very small, cf. also [34]. This description was applied in [31] representing the un-integrated gluon density by

$$f_g(x,k^2) = \widetilde{f}_g^{(0)}(x,k^2) + \overline{\alpha}_s(k^2)\left[k^2 \mathbf{L}[f_g,k_0^2]\right] + \left(\frac{x}{6}P_{gg}(x) - 1\right)$$
$$\otimes \int_{k_0^2}^{k^2} \frac{dk'^2}{k'^2} f_g(x,k'^2) + \frac{\alpha_s(k^2)}{2\pi} \int_x^1 dz P_{gq}(z) \Sigma\left(\frac{x}{z},K^2\right) . \quad (4)$$

Here $\mathbf{L}$ denotes the Lipatov kernel with a lower cut-off and $\widetilde{f}_g^{(0)}$ is the modified inhomogeneous term. A good fit to the F_2 data was obtained using a flat input distribution for the gluon, cf. [31].

In the conventional approaches, the QCD evolution equations are considered for parton densities

$$\frac{d}{d\log Q^2}\left(\begin{array}{c} \Sigma(N,Q^2) \\ G(N,Q^2) \end{array}\right) = \left(\begin{array}{cc} P_{qq} & P_{qG} \\ P_{Gq} & P_{GG} \end{array}\right)(N,\alpha_s) \otimes \left(\begin{array}{c} \Sigma(N,Q^2) \\ G(N,Q^2) \end{array}\right), \quad (5)$$

and are thus renormalization and factorization scheme dependent. Already in refs. [35] the study of evolution equations for observables has been proposed. These equations are scheme independent and their accuracy is only determined by the order in α_s which is accounted for. Recently this approach was followed in refs. [36,37] choosing F_2 and F_L as the observables and including the LO small x resummed anomalous dimensions into the analysis. Eqs. (5) may be transformed into evolution equations for F_2 and F_L eliminating the singlet and gluon distributions by using

$$F_2^S = c_2^S \Sigma + c_2^g G$$
$$F_L^S = c_L^S \Sigma + c_L^g G, \quad (6)$$

from which

$$\frac{d}{d\log Q^2}\left(\begin{array}{c} F_2^S(N,Q^2) \\ \hat{F}_L^S(N,Q^2) \end{array}\right) = \left(\begin{array}{cc} P_{22} & P_{2L} \\ P_{L2} & P_{LL} \end{array}\right)(N,\alpha_s) \otimes \left(\begin{array}{c} F_2^S(N,Q^2) \\ \hat{F}_L^S(N,Q^2) \end{array}\right) \quad (7)$$

is obtained, where $\hat{F}_L^S = (2\pi/\alpha_s)F_L^S$, and N denotes Mellin index. As a result of the LO + LO $\log(1/x)$–study [37] a lower χ^2 value was found than

in different NLO analyses of the structure function $F_2(x,Q^2)$. This applies particularly to the range $x \leq 0.1$, whereas for $x > 0.1$ the χ^2 was somewhat larger than in the NLO analysis.

Extending earlier analyses [38] the effect of the N_f terms in the small x resummed anomalous dimension $\gamma_{gg}(N)$, which was recently calculated in ref. [39], was investigated for the evolution of $F_2(x,Q^2)$ in [40]. In the DIS$-\overline{\rm MS}$ scheme the contribution to $F_2(x,Q^2)$ is positive but suppressed by at least a factor of 30 w.r.t. the value of $F_2(x,Q^2)$ accounting for the resummed quark anomalous dimensions in NLO. The small x resummed contributions for $F_L(x,Q^2)$ and $F_2^\gamma(x,Q^2)$ were also studied in [38]. For $F_2^\gamma(x,Q^2)$ the resummation effect on the photon-specific inhomogeneous solution originates solely from the resummed homogeneous evolution operator. Since the input densities are harder if compared to the proton case the small x resummed terms emerge already in the range $x \sim 10^{-2}$.

α_S IN DEEP INELASTIC SCATTERING

One of the most important theoretical achievements reported at this conference is the 4–loop calculation of the β function of QCD in the $\overline{\rm MS}$ scheme [41], which determines the evolution equation for $a_s = \alpha_s/(4\pi)$

$$\frac{\partial a_s}{\partial \ln \mu^2} = -\beta_0 a_s^2 - \beta_1 a_s^3 - \beta_2 a_s^4 - \beta_3 a_s^5 + O(a_s^6) \; . \tag{8}$$

Herewith a further step on the way to put QCD to the ultimate test has been performed. As already in the case of the 2–loop result [42] the calculation of the renormalized strong coupling is most easily carried out considering the renormalization of the ghost-ghost-gluon vertex,

$$g_{s0} = \frac{\widetilde{Z}_1}{\widetilde{Z}_3} \frac{1}{\sqrt{Z_3}} g_s \; . \tag{9}$$

The calculation still involves 30 834 vertex and 21 128 self-energy diagrams. For $SU(3)_c$, where $C_A = 3, C_F = 4/3, T_R = 1/2$, the expansion coefficients in eq. (8) read

$$\beta_0 = \frac{1}{4}\left[11 - \frac{2}{3}N_f\right] \tag{10}$$

$$\beta_1 = \frac{1}{16}\left[102 - \frac{38}{3}N_f\right] \tag{11}$$

$$\beta_2 = \frac{1}{64}\left[\frac{2857}{2} - \frac{5033}{18}N_f + \frac{325}{54}N_f^2\right] \tag{12}$$

$$\beta_3 = \frac{1}{256}\left[\left(\frac{149753}{6} + 3564\zeta_3\right) - \left(\frac{1078361}{162} + \frac{6508}{27}\zeta_3\right) N_f \right. \\ \left. + \left(\frac{50065}{162} + \frac{6472}{81}\zeta_3\right) N_f^2 + \frac{1093}{729}N_f^3\right] \; . \tag{13}$$

In 4–loop order new color coefficients do emerge, as well as β_3 turns out to be transcendental in the $\overline{\rm MS}$ scheme, unlike the case of the lower coefficients. Recently an attempt has been made to predict β_3 on the basis of the lower expansion coefficients and a known constraint applying the Pade approximation [43]. The latter result differs from the complete calculation, which is partly caused by the emergence of new color factors.

New results were also presented on the 3–loop corrections of the Ellis-Jaffe sum rule [44]

$$\begin{aligned}\int_0^1 dx g_1^{p(n)}(x) = &\left[1 - \left(\frac{\alpha_s}{\pi}\right) - 3.583\left(\frac{\alpha_s}{\pi}\right)^2 - 20.215\left(\frac{\alpha_s}{\pi}\right)^3\right] \\ &\times \left[\pm\frac{1}{12}|g_A| + \frac{1}{36}a_8\right] \\ &+ \left[1 - 0.333\left(\frac{\alpha_s}{\pi}\right) - 0.550\left(\frac{\alpha_s}{\pi}\right)^2 - 4.447\left(\frac{\alpha_s}{\pi}\right)^3\right]\frac{\hat{a}_0}{9}\ , \qquad (14)\end{aligned}$$

where $|g_A| = \Delta u - \Delta d, a_8 = \Delta u + \Delta d - 2\Delta s$, $a_0 = \Delta u + \Delta d + \Delta s$, and $\hat{a}_0 = \exp[-\int^{a_s(\mu^2)} da'_s \gamma^s(a'_s)/\beta(a'_s)]a_0(\mu^2)$. They may become important in later QCD analyses, when much more precise measurements of $g_1^{p(n)}(x,Q^2)$ will be available in the future.

In a recent QCD analysis the CCFR collaboration has performed a measurement of the strong coupling constant [45] obtaining

$$\alpha_s^{\rm NLO}(M_Z^2) = 0.119 \pm 0.002({\rm exp}) \pm 0.001({\rm HT}) \pm 0.004({\rm scale})\ . \qquad (15)$$

This value is larger than that obtained in an earlier measurement, $\alpha_s^{\rm NLO}(M_Z^2) = 0.111 \pm .002 \pm .003$, by the same experiment and other values measured in different deep inelastic scattering experiments, though being compatible within the experimental errors, see figure 5. The largest theoretical uncertainty is due to the renormalization and factorization scale, whereas uncertainties due to higher twist effects (HT) are estimated to contribute only marginally. The NuTeV neutrino experiment, which is currently running at the Tevatron, will allow a number of improvements to the analysis. There is a sign-selected beam, which should increase anti-neutrino statistics, and a continuous test beam which will allow a better determination of the hadron and muon energy calibrations and resolutions, currently being the largest experimental contributions to the systematic uncertainty.

$\alpha_s(M_Z^2)$ was also determined in a NLO QCD analysis of the polarized structure function $g_1(x,Q^2)$, [46], yielding

$$\alpha_s^{\rm NLO}(M_Z^2) = 0.120 \begin{array}{cc|cc} +0.004 & & +0.009 & \\ -0.005 & |_{\rm exp} & -0.006 & |_{\rm thy} \end{array}\ . \qquad (16)$$

Further determinations of α_s were reported using the GLS sum rule

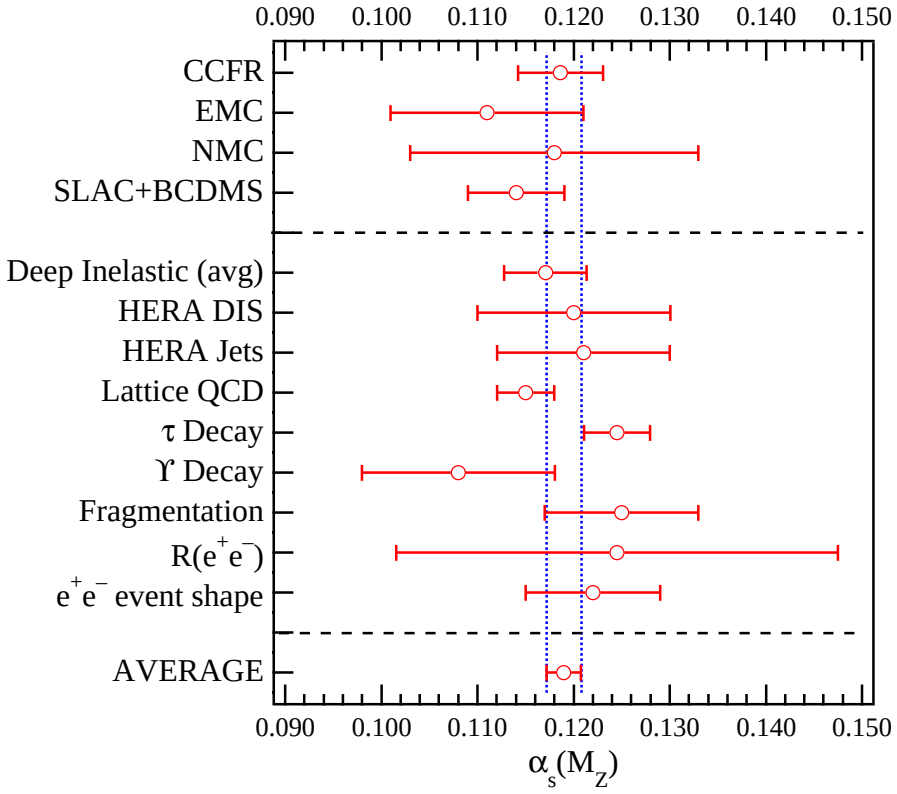

Figure 5 : A comparison of different measurements of $\alpha_s(M_Z^2)$, [45].

$$\int_0^1 dx F_3(x,Q^2) = 3\left[1 - \frac{\alpha_s}{\pi} - a\left(\frac{\alpha_s}{\pi}\right)^2 - b\left(\frac{\alpha_s}{\pi}\right)^3\right] - \Delta\mathrm{HT}, \tag{17}$$

and the polarized Bjorken sum rule

$$\int_0^1 dx \left[g_1^p(x,Q^2) - g_1^n(x,Q^2)\right] = \frac{|g_A|}{6}\left[1 - \frac{\alpha_s}{\pi} - 3.583\left(\frac{\alpha_s}{\pi}\right)^2 - 20.215\left(\frac{\alpha_s}{\pi}\right)^3\right]. \tag{18}$$

As a (preliminary) result CCFR obtained [45]

$$\alpha_s^{\mathrm{NLO}}(M_Z^2) = 0.112 \;\; {}^{+0.004}_{-0.005}\Big|_{\mathrm{stat}} \;\; {}^{+0.006}_{-0.005}\Big|_{\mathrm{syst}} \;\; {}^{+0.004}_{-0.005}\Big|_{\mathrm{HT}} \pm 0.008 \;\; (\mathrm{Model}) \tag{19}$$

with a lower central value than found in the global QCD analysis, eq. (15).

From the Bjorken sum rule, eq. (18), $\alpha_s(M_Z^2)$ was determined in [46] as

$$\alpha_s^{\rm NLO}(M_Z^2) = 0.118\ {}^{+0.010}_{-0.024} \tag{20}$$

with larger errors than in the QCD analysis of $g_1(x,Q^2)$ itself, mainly due to the uncertainty in the low x extrapolation.

The future prospects to measure α_s from the scaling violations of the structure function $F_2^{ep}(x,Q^2)$ were also discussed in a contribution to this workshop [47,20]. In a detailed numerical comparison four independent NLO evolution codes were found to agree by better than $\pm 0.05\%$ for the kinematic range of HERA [48]. Due to this the algorithmic uncertainty in the measurement of α_s is well under control.

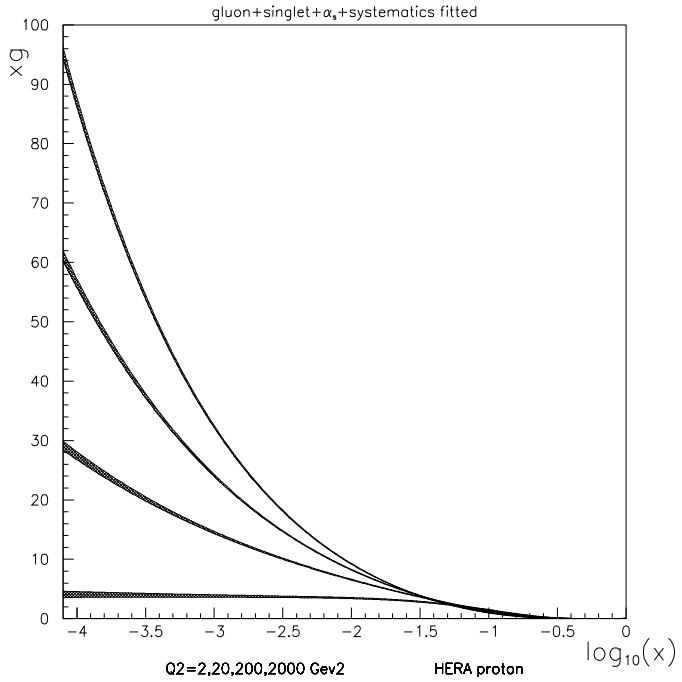

Figure 6: The gluon distribution versus x for different values of Q^2 obtained from a fit to simulated high energy HERA proton data. The bands show the total error.

For an integrated luminosity of $\mathcal{L} = 500 pb^{-1}$ $\alpha_s(M_Z^2)$ may be measured in the HERA range with experimental errors of

$$\delta\alpha_s^{\rm NLO}(M_Z^2) = 0.0025...0.0035 \quad \text{(systematics fixed)} \tag{21}$$
$$\delta\alpha_s^{\rm NLO}(M_Z^2) = 0.0015...0.0020 \quad \text{(systematics fitted)}\ . \tag{22}$$

A considerable improvement can be obtained fitting systematic effects. The constraints which can be derived for the gluon density in the latter case are illustrated in figure 2 for an integrated luminosity of $\mathcal{L} = 500 pb^{-1}$.

The theoretical errors of different kind for the α_s measurement were analyzed in [49]. The largest contributions are due to the use of NLO relations for α_s differing in NNLO,

$$\Delta\alpha_s^{\rm NLO}(M_Z^2) = 0.003 \quad \text{(representation of } \alpha_s\text{)}, \tag{23}$$

and the renormalization and factorization scale uncertainties,

$$\Delta\alpha_s^{\rm NLO}(M_Z^2) = \pm 0.005 \text{ (ren.)} \pm 0.003 \text{ (fact.)} \qquad (Q^2 > 50 \text{ GeV}^2). \tag{24}$$

Because these errors are larger than the expected experimental errors one would wish to be able to perform a NNLO analysis, in which these uncertainties become smaller. For this, the 3–loop splitting functions have yet to be calculated.

DIRECT PHOTONS

A comparison of direct photon data from a number of experiments to NLO QCD predictions reveals [50–52] a pattern of systematic deviations that cannot be reproduced by any modification to the parton distributions, see Figure 7. One possible explanation for the deviations is that they are due to soft gluon emissions, i.e. k_T effects, similar to those encountered in Drell-Yan production. In the latter case, a complete description of the soft gluon effects requires a resummation-type calculation.

The effects can be approximated using a Gaussian smearing procedure and/or parton shower Monte Carlo programs. Soft gluon emission steepens the direct photon cross sections at low transverse momentum and, in the case of fixed target direct photon experiments, changes the normalization. The value of the k_T can be measured directly in diphoton production, as in the Drell-Yan process, and by measuring the properties of the away-side jet in direct photon production [51]. The theoretical expectation is that the average value of the k_T should increase roughly logarithmically with the center of mass energy.

A complete description of direct photon data, especially at fixed target energies, may await a complete resummation calculation of the cross sections. Preliminary work in that direction has already taken place [53]. As an intermediate step, Baer and Reno [54] have added parton showering to a NLO photon production calculation and have shown that it is possible to describe the rise observed at low p_T in CDF at both $\sqrt{s} = 1800$ GeV and $\sqrt{s} = 630$ GeV [55].

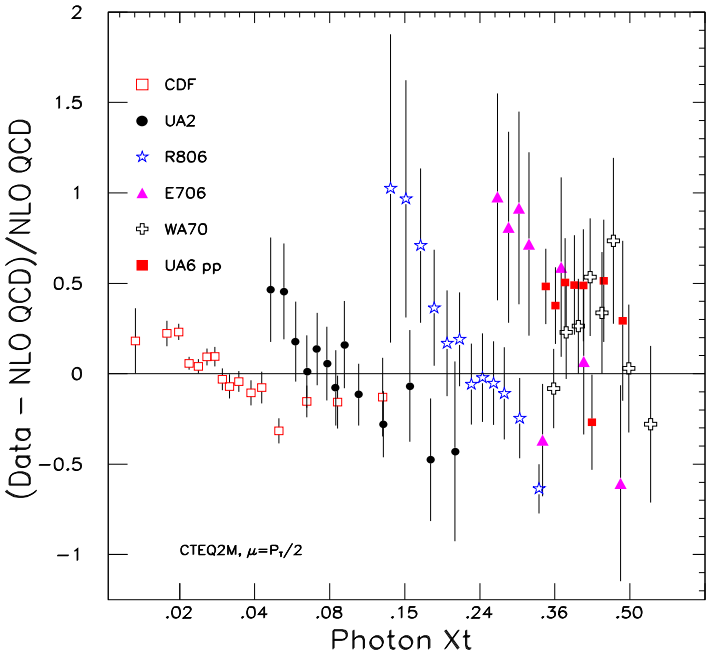

Figure 7: The quantity (Data-Theory)/Theory plotted vs x_T for a number of direct photon experiments. Theory corresponds to NLO order QCD with CTEQ2M parton distribution functions.

Previous common wisdom held that fixed target direct photon data served to fix the gluon distribution in the proton, since the dominant mechanism for prompt photon production in proton-proton collisions is gluon-quark scattering. However, the k_T effects mentioned above, and the residual scale-dependence at NLO of the direct photon theory, can affect both the slope and normalizations of the cross sections.

An attempt has been made to incorporate the fixed target direct photon data from the Fermilab experiment E706 [51] into the CTEQ global fitting program, first correcting for the soft-gluon (k_T) effects. The direct photon data probe the gluon distribution up to very high values of $x \sim 0.7$. The gluon distribution obtained from the fit agrees well with that from CTEQ4M. The average k_T values used (1.15 GeV/c at $\sqrt{s} = 31.5$ and 1.30 GeV/c at 38.7 GeV) agree with the k_T values measured in Drell-Yan experiments in similar kinematic regimes and with the direct determination of the event k_T from the E706 data. The k_T-corrected cross sections describe well the slope and the normalization of the data, even at the highest values of x.

THE HIGH Q^2 RANGE

Jet Rates at the Tevatron

The jet production at the Tevatron serves as a crucial venue for the measurement of the gluon distribution, the determination of α_s, and probing of parton distributions at highest x and Q^2 values [50].

The leading order cross sections for jet production are proportional to α_s^2, and to $G^2(x,Q)$ for gluon-gluon scattering, $G(x,Q)Q(x,Q)$ for gluon-quark scattering, and $Q(x,Q)Q(x,Q)$ for quark-quark scattering. In the mid-range of the inclusive central jet data, $50\,\mathrm{GeV} < E_T < 200\,\mathrm{GeV}$, gg and gq scattering dominate. This is a region where systematic errors, both theory and experiment, are smallest and where the theory agrees well with the data. The CDF and D0 cross sections are also within relatively good agreement within this range [50,56]. At high values of E_T, CDF has reported an excess over standard theoretical predictions.

The CDF [57] and D0 [58] jet data have been included in a global parton distribution analysis (CTEQ4M) [22]. The jet inclusive data serve to stabilize the fits and to constrain the gluon distribution in the x range from 0.05 to 0.22. The inclusive jet data prefer a value of α_s of 0.116 to 0.118, consistent with the global fit results.

As mentioned previously, CDF has reported an excess in the inclusive cross section at the highest values of transverse energy. This may be due to new physics or to a possible modification of the parton distributions [59]. The quark distributions in the x and Q^2 range $(0.4 - 0.5, 1 - 2 \times 10^5\,\mathrm{GeV}^2)$ corresponding to high E_T central jet production are fairly well-constrained, but there is greater flexibility and uncertainty in the gluon distribution. This freedom is largely due to two sources: the theoretical uncertainties in fixed target direct photon production and the lack of other data in current global fits to constrain the gluon distribution at high x.

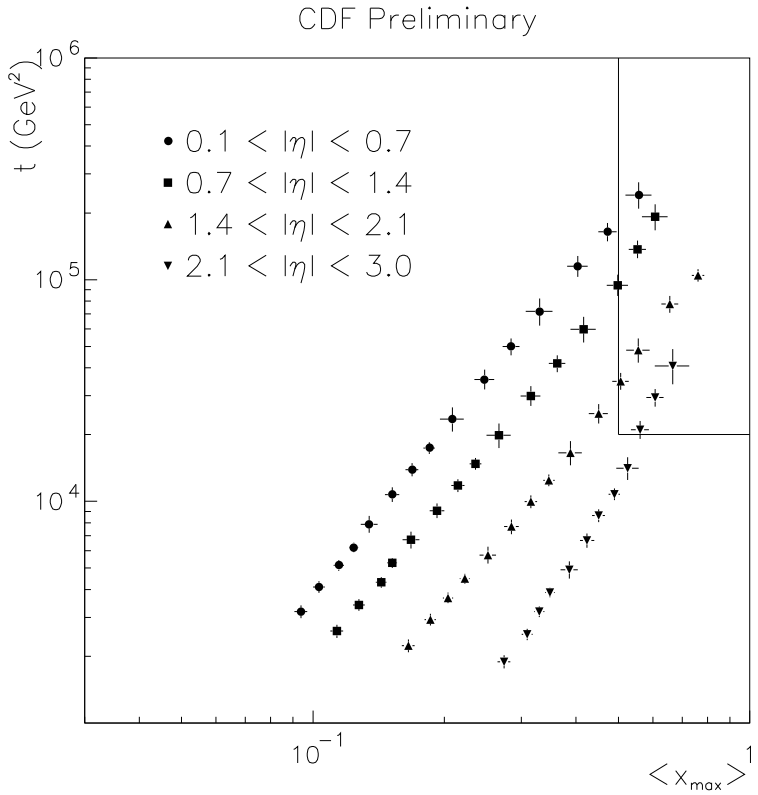

Figure 8: The momentum-transfer-squared (t) plotted as a function of the larger of the x values in the parton-parton collision for the CDF differential dijet cross section. The box indicates the region of the HERA excess.

One cannot conclude that the excess is due to gluons, just that the data currently used in the global fits allow for a description of the excess by a larger gluon distribution. No definite conclusions can be drawn about the larger gluon distribution without the use of additional data. Note also that since the dominant jet production mechanism in this E_T range is quark-quark scattering, any appreciable modification to the jet cross section requires a much larger modification of the gluon distribution.

This exercise with the high E_T jet distribution also points out the need for flexibility in the parameterization of parton distributions, especially when extrapolating to new regions of x and Q^2 [50,60].

One can specifically probe high values of x by measuring the differential dijet cross section. In the CDF differential dijet analysis [56], one jet (the trigger jet) is required to be central ($0.1 < |\eta| < 0.7$) while the other jet (the probe jet) is allowed to have an $|\eta|$ value of up to 3. The trigger and probe jets are the two highest E_T jets in the event.

High E_T scatters in which the probe jet is at high rapidity correspond to collisions of a parton at moderate x (0.05–0.3) with a high x parton (up to $x \sim 0.75$) at very high Q^2 (up to 10^5 GeV^2). The x and Q^2 values probed over-

lap (and in some cases exceed) those in the HERA high x and Q^2 analysis, as shown in Figure 8. Any modifications to the parton distributions to explain the HERA high x and Q^2 results [60] would have a similar impact on the differential dijet data. The data should also serve to test the hypothesis of a larger gluon at high x. One complication is that for large trigger jet E_T values and high probe jet rapidities, the cross section is dominated by multijet final states due to the larger phase space. One either needs to compare to higher order calculations or to measure the cross sections as a function of the parton light-cone momentum fractions X_A and X_B, and the dijet pseudorapidity difference η^*, as suggested by Ellis and Soper [61]. A measurement of this type should be less sensitive to higher order corrections and should provide a more definitive statement on the parton distributions at high x and Q^2.

Event Rates at HERA

The ZEUS and H1 experiments have reported on an excess of events above standard model predictions at high Q^2 and large values of x [62,63]. With a total luminosity of 14 pb^{-1}, H1 found 12 events above Q^2 of 15000 GeV^2 where 4.7 events are expected. ZEUS found 4 events for $x > 0.55$ and $y > 0.25$ where 0.9 events are expected. A quantitative comparison of the distributions from the two experiments is not possible since the resolution effects are not the same for the two data sets. The uncertainties in the Standard Model predictions are dominated by the uncertainties in the structure functions, measured at fixed target experiments and evolved to high Q^2. This uncertainty is at the level of 5–7% [20,62,63] in case that the conventional parametrizations of the parton distributions are used.

The H1 collaboration has determined the probability that there is a statistical fluctuation of the same or larger magnitude as observed at $Q^2 > 15000$ GeV^2 to amount 0.006. Similarly the ZEUS collaboration finds this probability for the region $x > 0.55$ and $y > 0.25$ to be 0.0072.

Phenomenological Aspects

Shortly after the publication of the excess of events in the high Q^2 range by both the H1 and ZEUS experiments [62,63] a series of theoretical and phenomenological studies was carried out seeking for possible interpretations [64]. The observed excess was neither predicted nor do we have a thorough theoretical concept to explain it currently. During this workshop interpretations as due to single leptoquark production [65], effects due to R-parity violating supersymmetry [66], the presence of contact terms [67], and others [68], as well as uncertainties in the knowledge of the structure functions at larger values of x [60] and consequences for e^+e^- experiments [69] were discussed.

The Tevatron experiments reported on constraints which have been derived by them for the leptoquark pair production cross section [70].

Leptoquarks

If the observed high-Q^2 excess is interpreted in terms of single leptoquark production constraints on the fermionic couplings λ of the leptoquarks Φ, which may be either scalars or vectors, may be derived. Due to the location of the excess found by H1 in the range $M = \sqrt{xS} \sim 200$ GeV we assume this scale in some of the estimates being considered below. In the narrow width approximation the production cross section reads

$$\sigma = \frac{\pi^2}{2}\alpha \left(\frac{\lambda}{e}\right)^2 q(x, \langle Q^2 \rangle) \left\{ \begin{array}{ccc} 2 & : & V \\ 1 & : & S \end{array} \right. \times Br(\Phi \to eq) \; . \tag{25}$$

For the observed excess in the $e^+ + jet$ channel at H1

$$\frac{\lambda_S}{e}\sqrt{Br} \sim 0.075 \;\; (0.15) \qquad u \;\; (d), \qquad \Phi = S \tag{26}$$

is derived, cf. [65,71][2], while $\lambda_V = \lambda_S/\sqrt{2}$ and $\lambda_{\rm ZEUS} = 0.55\lambda_{\rm H1}$. These couplings are well compatible with the limits derived from low energy data [73]. An information on the spin of the produced state can be derived from the y distribution of the events. The statistics is yet to low to allow for such a detailed analysis, however, one may compare the average values. For the H1 events one obtains $\langle y \rangle_{\rm H1} = 0.59 \pm 0.02$, which is compatible with both the expectation for a scalar $\langle y \rangle_S = 0.65$ or a vector $\langle y \rangle_V = 0.55$, cf. [71].

A severe constraint on the leptoquark states which may be produced in e^+q scattering is imposed by their $SU(2)_L \times U(1)_Y$ quantum numbers[3]. If besides the e^+q final states the indication of also νq final states becomes manifest, no scalar leptoquarks are allowed since low energy constraints demand either $\lambda_L \ll \lambda_R$ or $\lambda_R \ll \lambda_L$. In this case only the vectors $U^0_{3\mu}$ or $U_{1\mu}$, which may be produced in the e^+d channel, are allowed. For these states the branching ratios are $Br(e^+d) = Br(\nu u) = 1/2$. If the observed excess turns out to be due to single leptoquark production also $e(\nu) + 2jet$ final states have to be observed with $M_{e(\nu)+jet} \sim 200\,{\rm GeV}$ [75].

Experimental constraints on the existence of leptoquarks in the mass range $M \sim 200\,{\rm GeV}$ can be derived from the Tevatron data for the leptoquark pair production cross section [76]. Results of this analysis were reported in [70]. The current bounds[4] for leptoquarks associated to the 1st fermion family are [70] :

---

[2] Earlier references on the phenomenology of leptoquarks may be found in [65,71,72].

[3] For a classification in the case of family-diagonal, baryon- and lepton number conserving, non-derivative couplings, see [74].

[4] At the time of the workshop the bounds were lower by 35 GeV.

$$
\begin{aligned}
&M_S < 210 \ \text{GeV}, && Br(eq) = 1 && (95\%\ CL) \\
&M_S < 190\ (225\ \text{GeV}), && Br(eq) = 0.5\ (1) && (95\%\ CL). \qquad (27)
\end{aligned}
$$

The corresponding limits for vector leptoquarks are expected to be larger [76], since the pair production cross section is larger by a factor of at least 2...3 for a factorization mass of $\mu = M_\Phi$ [71]. Whereas leptoquarks with $Br(eq) = 1$ are ruled out at 95% CL by the Tevatron bounds, those with $Br(eq) = 0.5$ are still (marginally) allowed.

R-parity violating SUSY

Supersymmetric theories with R-parity breaking bear also scalar leptoquark states [66]. The tight bounds from Tevatron for states with $Br(eq) = 1$ do not apply to this class of leptoquarks since the cascade decays contain a light (unvisible) supersymmetric particle in the final state. Among the different possible states $\tilde{u}_L$ is excluded due to limits from $\beta\beta$ decay. $\tilde{c}_L$ is allowed and would lead to a contribution to $Br(K^+ \to \pi^+ \nu\overline{\nu})$ close to the current bound on this process. Both the processes $e^+ d \to \tilde{t}_L$ and $e^+ s \to \tilde{t}_L$ are allowed at a sufficient production rate.

Contact Interactions

Since part of the current high Q^2 events are distributed in a somewhat wider range one might as well try to describe them with the help of an effective Lagrangian containing contact interactions at some scale Λ,

$$
L_{eff} = \sum_{q=u,d} \sum_{h_1,h_2=L,R} \eta^{eq}_{h_1,h_2} \overline{e}_{h_1} \gamma^\mu e_{h_1} \overline{q}_{h_2} \gamma_\mu q_{h_2}, \qquad (28)
$$

with

$$
\eta^{eq}_{h_1,h_2} = \pm \frac{4\pi}{\Lambda^2_{h_1,h_2}}, \qquad [\Lambda] = \ \text{GeV} \ . \qquad (29)
$$

Various of the possible interactions described by (28) are already well constrained. e^+p interactions are particularly sensitive to the η_{LR} and η_{RL} terms [67], which could provide a description with Λ being of $O(3\ \text{TeV})$.

Uncertainties of parton densities at larger x

Both the H1 and ZEUS collaborations estimated the uncertainty of the quark densities in the range $x \sim 0.4...0.5$, in which the excess of events is observed to be of $O(5-7\%)$. As well–known, the parton densities are not yet well constrained experimentally at very large x, $x \gtrsim 0.8$. A feed–back of this uncertainty into the range of lower x values in QCD fits is not excluded and

was studied in [60] under a series of assumptions. Although more studies are needed the above mentioned uncertainty is essentially confirmed and the excess of events cannot be attributed to an uncertainty in the parton densities currently.

Implications for e^+e^- scattering

The fermionic couplings of leptoquark states in the mass region $M \sim 200\,\mathrm{GeV}$ may be probed in e^+e^- scattering searching for a possible interference of leptoquark exchange in the t-channel and $\gamma - Z$ exchange in the s-channel. The corresponding effects at SLC, LEP1 and LEP2, however, are smaller than 1% [77,69] assuming the couplings (26) and can thus not be detected for leptoquarks in this mass range. On the other hand, LEP2 may constrain related contact interaction terms up to scales of $\Lambda \gtrsim 4...6.5\,\mathrm{TeV}$ [69] on the basis of the data being accumulated until the end of this year. Furthermore one may as well search for some specific signatures associated to leptoquarks which emerge in scenarios with supersymmetric models with R–parity violation.

CONCLUSIONS

There has been considerable progress in the measurement of the deep inelastic scattering structure functions during the last year. With the increased luminosity, which will be collected by the HERA experiments until DIS '98, the precision to which $F_2(x,Q^2)$ and $F_2^{c\bar{c}}$ will be determined will be higher and allow for even more detailed comparisons with the theoretical predictions. With the availability of the complete small x resummed anomalous dimension γ_{gg} a more complete analysis of the small x behavior of $F_2(x,Q^2)$ can be performed. To be able to analyze also the behavior of the structure functions for lower values of Q^2 the twist–4 anomalous dimensions need to be known.

The most exciting question is certainly whether or not the excess of neutral current events in the high Q^2 region of HERA will persist adding in the data of the 1997 runs, and whether such an excess is also present in the charged current data. This question will be answered before DIS '98 by the HERA experiments. If a clear manifestation of new physics will be found, will we have the theory for it in a year from now?

Acknowledgement. We would like to thank all the speakers for their contributions to the working group. Our thanks are also due to M. Derrick, D. Krakauer, J. Repond, and the other members of the organizing committee of DIS '97 for organizing a very fruitful meeting in a splendid atmosphere.

REFERENCES

1. B. Surrow in these proceedings.

2. A. Meyer in these proceedings.
3. E. Kabuss in these proceedings.
4. R. Bernstein in these proceedings.
5. F. Zomer in these proceedings.
6. H1 Coll., C. Adloff et al., *Phys. Lett.* **B393** 452 (1997).
7. H1 Coll., S. Aid et al., *Nucl. Phys.* **B470** 3 (1996).
8. ZEUS Coll., M. Derrick et al., *Z. Phys.* **C72** 399 (1996).
9. A. Donnachie and P.V. Landshoff, *Z. Phys.* **C61** 139 (1994).
10. M. Glück et al., *Z. Phys.* **C67** 433 (1995).
11. P.Z. Quintas et al., *Phys. Rev. Lett.* **71** 1307 (1993).
12. NMC Coll., M. Arneodo et al., *Nucl. Phys.* **B483** 3 (1997).
13. J. Blümlein et al., in : Proc. of the HERA Workshop, ed. R.D. Peccei, (DESY, Hamburg, 1988), **Vol. 1**, p. 67;
    M. Cooper-Sarkar et al., in : Physics at HERA, Proc. of the Workshop, eds. W. Buchmüller and G. Ingelman (DESY, Hamburg, 1992) p. 155.
14. L. Bauerdick et al., in : Future Physics at HERA, Proc. of the Workshop, eds. G. Ingelman, A. De Roeck, and R. Klanner, (DESY, Hamburg, 1996) p. 77.
15. M. Krasny et al., in : Physics at HERA, Proc. of the Workshop, eds. W. Buchmüller and G. Ingelman (DESY, Hamburg, 1992) p. 171.
16. L. Favart et al., *Z. Phys.* **C72** 425 (1996).
17. C. Royon, these proceedings; H. Navelet et al., *Phys. Lett.*, **B385**, 357 (1996), and references therein.
18. H1 Coll., C. Adloff et al., *Z. Phys.* **C72** 593 (1996).
19. J. Roldán, these proceedings; ZEUS Collaboration, J. Breitweg et al., DESY 97-089, submitted to *Z. Phys.* **C**.
20. M. Botje, these proceedings.
21. E. Laenen et al., *Phys. Lett.* **B291** 260 (1990); *Nucl. Phys.* **B374** 36 (1992).
22. H. Lai, these proceedings; H. Lai et al., *Phys. Rev.* **D55** 1280 (1997).
23. R.G. Roberts, these proceedings `hep-ph/9706269`; A.D. Martin et al. `hep-ph/9612449`.
24. H. Lai and W.K. Tung, *Z. Phys.* **C74** 463 (1997) and references therein;
25. M. Buza et al., `hep-ph/9612398`.
26. M. Buza and W.L. van Neerven, `hep-ph/9702242`.
27. C. Schmidt, these proceedings `hep-ph/9706469`; F. Olness, these proceedings.
28. D. Haidt, these proceedings.
29. W. Buchmüller and D. Haidt, `hep-ph/9605428`.
30. B. Badelek, these proceedings.
31. J. Kwiecinski et al., these proceedings `hep-ph/9706445` and `hep-ph/9703445`.
32. A. Askew et al., *Phys. Rev.* **D47** 3775 (1993).
33. J. Blümlein, *J. Phys.* **G19** 1695 (1993).
34. J. Blümlein, *Nucl. Phys.* **B** *(Proc. Suppl.)* **39B,C** 22 (1995).
35. L. Baulieu and C. Kounnas, *Nucl. Phys.* **B155** 429 (1979);
    W. Furmanski and R. Petronzio, *Z. Physik* **C11** 293 (1982);
    M. Glück, E. Hoffman, and E. Reya, *Z. Physik* **C13** 119 (1982).
36. S. Catani, *Z. Phys.* **C70** 263 (1996).

37. R. Thorne, these proceedings, hep-ph/9706233; *Phys. Lett.* **B392** 463 (1997); hep-ph/9701241.
38. J. Blümlein et al., hep-ph/9608470, *Nucl. Phys.* **B** (*Proc. Suppl.*) **51C** 30 (1996).
39. G. Camici and M. Ciafaloni, *Phys. Lett.* **B386** 341 (1996), and in preparation.
40. J. Blümlein and A. Vogt, these proceedings, hep-ph/9706371; J. Blümlein and A. Vogt, DESY 96–096.
41. T. van Ritbergen, these proceedings;
    S. Larin et al., hep-ph/9701390.
42. O. Tarasov et al., *Phys. Lett.* **B93** 429 (1980);
    S. Larin and J. Vermaseren, *Phys. Lett.* **B303** 334 (1993).
43. J. Ellis et al., hep-ph/961202.
44. S. Larin et al., hep-ph/9702435.
45. P. Spentzouris, these proceedings;
    CCFR collaboration, W. Seligman et al., hep-ex/9701017.
46. G. Ridolfi, these proceedings, G. Altarelli et al., hep-ph/9701289.
47. M. Botje et al., in: Future Physics at HERA, Proc. of the 1996 Workshop, eds. G. Ingelman, A. DeRoeck, and R. Klanner, (DESY, Hamburg, 1996), p. 33.
48. J. Blümlein et al., in: Future Physics at HERA, Proc. of the 1996 Workshop, eds. G. Ingelman, A. DeRoeck, and R. Klanner, (DESY, Hamburg, 1996), p. 23, hep-ph/9609400.
49. J. Blümlein et al., *Nucl. Phys.* **B** (*Proc. Suppl.*) **51C** 97 (1996), hep-ph/9608217.
50. J. Huston, these proceedings.
51. M. Zielinski, these proceedings.
52. J. Huston et al., *Phys. Rev.* **D51** 6139 (1995).
53. C.P. Yuan and G. Sterman, private communication.
54. H. Baer and D. Reno, *Phys. Rev.* **D54** 2017 (1996).
55. R. Blair, these proceedings.
56. F. Chlebana, these proceedings.
57. CDF Collaboration, *Phys. Rev. Lett.* **77** 438 (1996).
58. R. Hirosky, these proceedings.
59. J. Huston et al., *Phys. Rev. Lett.* **77** 444 (1996).
60. S. Kuhlmann, these proceedings; S. Kuhlmann et al., hep-ph/9704338.
61. S. Ellis and D. Soper, *Phys. Rev. Lett.* **74** 5182 (1995).
62. T. Carli, these proceedings; H1 collaboration, C. Adloff et al., *Z. Phys.* **C74** 191 (1997).
63. A.F. Zarnecki, these proceedings; ZEUS collaboration, J. Breitweg et al., *Z. Phys.* **C74** 207 (1997).
64. For a list of related references see ref. [65].
65. J. Blümlein, these proceedings, hep-ph/9706326 and references therein.
66. S. Lola, these proceedings, hep-ph/9706519 and references therein; G. Altarelli et al. hep-ph/ 9703276 and references therein; H. Dreiner and P. Morawitz hep-ph/9703279 and references therein.
67. D. Zeppenfeld, these proceedings, hep-ph/9706437 and references therein;

V. Barger et al., hep-ph/9703311.
68. A.R. White, these proceedings; hep-ph/9704248.
69. J. Kalinowski, these proceedings, hep-ph/9706203 and references therein; J. Kalinowski et al., *Z. Phys.* **C74** 595 (1997).
70. H.S. Kambara, CDF collaboration, Hadron Collider Physics XI, June 5–11 1997; G. Landsberg, D0 collaboration, Seminar, Fermilab, June 6 1997; G. Wang, these proceedings.
71. J. Blümlein, *Z. Phys.* **C74** 605 (1997).
72. J. Blümlein and E. Boos, *Nucl. Phys.* **B** *(Proc. Suppl.)* **37B** 181 (1994).
73. M. Leurer, *Phys. Rev. Lett.* **71** 1324 (1993), *Phys. Rev.* **D49** 333 (1994), *Phys. Rev.* **D50** 536 (1994); S. Davidson et al., *Z. Phys.* **C61** 613 (1994).
74. W. Buchmüller et al., *Phys. Lett.* **B191** 442 (1987).
75. J. Blümlein and A. Kryukov, DESY 97–067.
76. J. Blümlein et al., hep-ph/9610408, *Z. Phys.* **C** in print, and references therein.
77. A. Djouadi et al. SLAC–PUB–95–6772, hep-ph/9504210.